

Mechanically Programmable Dip Molding of High Aspect Ratio Soft Actuator Arrays

Kaitlyn P. Becker,* Yufeng Chen, and Robert J. Wood

This work presents multiple methods of creating high aspect ratio fluidic soft actuators that can be formed individually or in large arrays via dip coating. Within this methodology, four strategies are provided to mechanically program the motion of these actuators, including the use of fiber inclusions, gravity, surface tension, and electric fields. The modular nature of this dip coating fabrication technique is inexpensive, easy to modify, and scalable. These techniques are used to demonstrate the fabrication of soft actuators with aspect ratios up to 200:1 and integrated arrays of up to 256 actuators. Furthermore, these methods have the potential to achieve higher aspect ratios and larger array sizes. Operating pressure, curvature, and curling strength tests reveal the design space in which fabrication parameters can be selected to tune the input and output parameters of soft bending actuators. An individual bending actuator made with these methods weighs between 0.15 and 0.5 g, can hold up to 2 N, and can be designed to work in groups to increase curling strength with distributed contact forces. Arrays of these actuators may be useful in atypical grasping and manipulation tasks, fluid manipulation, and locomotion.

1. Introduction

Soft robots, typically composed of soft or compliant materials, demonstrate advantages over their rigid counterparts in gentle grasping and manipulation, passively adaptive mechanics, ability to achieve complex motions with relatively few inputs, and potential for safe human–robot interactions. These advantages are a benefit of their inherently high compliance and capacity for large deformations. However, this compliance also effectively limits the forces soft robots can apply to their environments. In this paper, we explore new fabrication

strategies that allow us to leverage the advantages that soft robots have to offer by maintaining low contact forces and creating large arrays of actuators that can work together to apply distributed forces, as well as high aspect ratio actuators that can deform in ways to create greater engagement with target objects. Arrays of high aspect ratio soft actuators can be valuable in applications involving fluid manipulation, locomotion, grasping, and delicate object manipulation. Fabrication of large arrays or high aspect ratios is challenging with many of the techniques being used to create soft actuators because it requires complex molds or the need to join many soft components together. In this work, we employ fabrication strategies based on modified dip-coating processes to address these challenges and build integrated soft actuator arrays as seen in **Figure 1**.


High aspect ratio actuator arrays can be leveraged in systems that emulate ciliary movement for the purpose of fluid mixing, fluid propulsion, general fluid manipulation, and low Reynolds number swimming. Test systems ranging from micrometer to millimeter scales have been fabricated by direct molding of actuators, casting into micromachined molds,^[1] casting into a deep-chemical etched silicon wafer molds,^[2] and casting into a multi-part precision molds with the help of capillary action to create one^[3] and two degree of freedom cilia arrays.^[4] Passive arrays of branching structures have been formed with a three part mold for the purpose of passive locomotion^[5] and similar methods could be used to create artificial ciliary systems. Larger arrays of smaller scale cilia structures have been demonstrated using a variety of alternative fabrication strategies including molding in a sacrificial filter that is later dissolved,^[6] self-assembly of magnetic particles,^[7] magnetic manipulation of rubber with embedded magnetic particles,^[8] and roll touch molding.^[9] Related work focused on ambulatory locomotion has also demonstrated the use of magnetic fields to form and later control large arrays of high aspect ratio structures from silicone filled with magnetic particles.^[8] Most of the arrays mentioned above are either passive structures, indirectly actuated by deformations in supporting structure, or manipulated via changes in a local magnetic field. The arrays created by Gorissen et al.^[3] and Milana et al.,^[4] however, are pneumatically actuated and the cilia are individually controllable.

Complementing fluid flow manipulation, a variety of high aspect ratio actuators have been made into tentacles and

K. P. Becker, Prof. Y. Chen, Prof. R. J. Wood
John A. Paulson School of Engineering and Applied Sciences
Harvard University
60 Oxford Street, Cambridge, MA 02138, USA
E-mail: kbecker@g.harvard.edu

K. P. Becker, Prof. Y. Chen, Prof. R. J. Wood
Wyss Institute for Biologically Inspired Engineering
Harvard University
3 Blackfan Circle, Boston, MA 02115, USA

Prof. Y. Chen
Research Laboratory of Electronics
Massachusetts Institute of Technology
Cambridge, MA 02138, USA

 The ORCID identification number(s) for the author(s) of this article can be found under <https://doi.org/10.1002/adfm.201908919>.

DOI: 10.1002/adfm.201908919

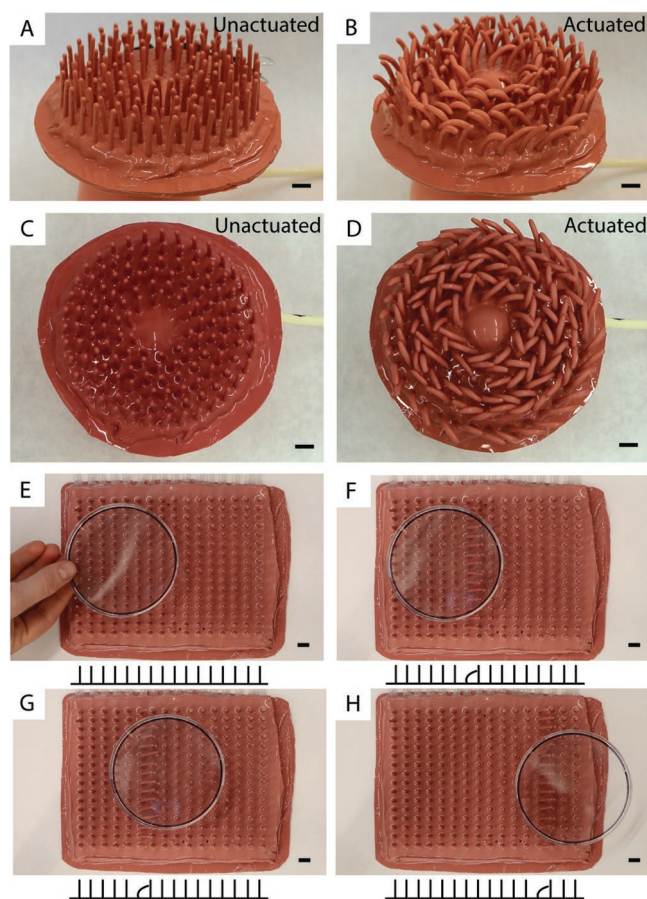


Figure 1. Examples of large arrays of structures made using open face molds. A–D) A 149-part array, mechanically programmed to bend in alternating clockwise and counterclockwise rings defined by the placement of fibers on the pins of an open face mold. E–H) A 256-part array of inflatable structures that are mechanically programmed to bend in the same direction using gravity augmented molding. Each column of 16 elements is controlled by a separate channel. E–H) A time lapse of a wave pattern moving through the actuator columns and pushing a petri dish. The pictures shown are from 0, 5, 15, and 104 s. The schematic below the images shows which column is being actuated. The scale bars in all images represent 1 cm.

miniature grippers for delicate grasping and manipulation of small, discrete objects. Corrugated microtentacles have been created by casting silicone rubber into a two part micromachined mold^[10] and also integrated into a three finger gripper.^[11] Moving away from traditional molding, bulk silicon fabrication techniques were used to create a four-fingered microgripper driven with pneumatic Parylene film balloons.^[12] Similarly, Parylene balloons have been used to create an array of bending actuators to emulate cilia capable of macroscale object manipulation.^[13] Researchers have also demonstrated casting PDMS into molds created with the use of MEMS fabrication techniques and stereo lithography to cast 2.5D components that are then bonded to construct microfingers^[14] and microactuators for retinal surgery.^[15] Arrays of similar actuators have then been integrated into a five-fingered microhand.^[16] Microfingers have also been fabricated with 2.5D molding that has been augmented to incorporate nanofiber strain-limiting inclusions,^[17]

similar to demonstrations of multimaterial actuators at larger scales.^[18–20] As a novel alternative to molding, a microtentacle gripper has been fabricated by dip coating a horizontal rod, using gravity to bias the wall thickness in the rubber coating that was formed around the rod. Once cured, the rod coating is removed, sealed on one end, and used as a soft pneumatic bending actuator.^[21] The fabrication methods presented in this paper are most closely related to our dip coating method and expand it further to larger arrays, longer actuators, and additional strategies to mechanically program a bending motion into the actuators.

In the above examples, high aspect ratio actuators with diameters ranging from micrometers to a few millimeters have been used for fluid flow manipulation, locomotion, and miniature grippers. Individual high aspect ratio actuators have been demonstrated in the form of continuum arms, tentacles, and tendrils for grasping and manipulation.^[22–26] Various other high aspect robots resembling worms and snakes have also been used to demonstrate locomotion.^[22] The individual gripping actuator that most closely resembles the dimensions and curling behavior of the actuators presented in this paper was created by Must et al., and their tendrill-like robot utilizes a novel reversible osmotic actuation that occurs on time scales of ≈ 1 h. Several macroscale applications have made use of arrays of high aspect ratio actuators. McKibben actuators can be made very long with relative ease and Kurumaya et al. bundled a group of thin, high aspect ratio McKibben actuators to be used as artificial muscles, demonstrating an array working together in place of a single actuator. The array achieves a greater system compliance while maintaining comparable composite strength to more traditional individual McKibben actuators of larger diameter.^[27] A different use of high aspect ratio features to incorporate compliance into a larger structure was explored by Zhou et al, who incorporated arrays of passive silicone pillars on the inner palm and finger surfaces of a soft robotic hand.^[28] The effect of these pillars can be compared to the memory foam used by Galloway et al. to minimize the (already low) stress concentration induced by soft grippers.^[29] Covering a soft robotic hand with macro-sized cilia can create a more gentle and robust grasp, where the compliant pillars conform to objects while offering lower resistance to shear deformations than memory foam.^[28] By introducing fabrication strategies to enable high aspect ratios and large arrays of actuable soft structures, we hope to contribute to this work of compliant structures that are able to provide distributed strength and manipulation capacity. This could be in the form of enhanced object grasping and manipulation with an active array of short pillars to augment the grasping concepts proposed by Zhou, larger arrays of macro cilia for fluid and object propulsion, or systems for locomotion.

The molds introduced in this work consist of inexpensive and modular laser-cut acrylic parts and commercially available stainless steel pins. In place of machining high precision interlocking mold parts, the mold components are assembled into a structure that is dipped into liquid rubber or poured over with liquid rubber. These open face molds define the internal part of the final geometry and the remaining (outer) geometry is entirely dictated by gravity, surface tension, and viscosity. These open face molds can be used to create functional soft

robotic actuators that are mechanically programmed to bend in the same uniform direction or to bend in an arbitrary predefined vector field of directions. As mentioned earlier, actuators made from a form of dip coating have also been demonstrated by Paek et al.^[21] We extend these principles to achieve higher aspect ratio actuators as well as larger arrays of actuators. Through the use of modular open face mold forms, we are able to rapidly and inexpensively make new molds, various sizes, and custom arrangements of soft actuators. We also introduce new strategies for mechanically programming the motion of these actuators, including modifications of familiar strategies such as fiber inclusions and gravity, as well as more novel strategies that make use of surface tension and electric fields. In this paper, we focus on the fabrication of actuable bending soft structures, or soft actuators, but the same techniques can be used to create passive soft structures.

2. Principles and Fabrication of Motion Programming Structures

The primary fabrication strategy presented in this work for the creation of high aspect ratios and large arrays of soft structures leverages the simplicity of open face molds. An example and schematic of how an open faced mold can be set up is shown in **Figure 2**. We are able to drastically reduce the complexity and tolerance requirements of the molds by relying on the balance of gravity, surface tension, and the rubber viscosity to determine the dimensions of the final structure, rather than requiring highly precise, multipart molds. This dipping or pour over technique mimics those used in the fabrication of dipped candles, latex balloons, and doctors' gloves, where the thickness of the resulting structure is not controlled by a precise mold but the rheology of the liquid applied.^[30]

The basic form used for the open faced molds in this work consisted of arrays of stainless steel pins press-fit into laser-cut acrylic plates, strips, and rings. Laser-cutter and acrylic plates were chosen for convenience but the molds could be made

via additive manufacturing, injection molding, milling, or even hand drilling in a variety of plastics or metal. In the work presented here, the use of laser-cut acrylic forms and commercially available pins allowed for easy creation of cut files and rapid, inexpensive construction of new molds. With standardized spacing, modular molds could be constructed with interchangeable parts for the purpose of reusing mold components as well as creating larger composite mold forms.

The general dip coating (or pour over) process used to make an array of actuators similar to those shown in Figures 1 and 2 begins with assembling an open face mold. The mold form is assembled onto a laser-cut acrylic base plate that fixes the relative positioning between components. Acrylic rings or bars are then placed on top of the base plate as rails that define the open channels that will supply fluid flow to the actuators. Rubber shims are cast in the region between the rails. Once cured, the acrylic fixture and rubber shims are pulled apart and then reassembled with fabric woven between the components, as shown in Figure 2. The pins that will define the interior dimension of the actuator are then press fit into holes going through the rails and base plate.

Before the first full dip coating of the open faced mold form, the tips of the pins are dipped into liquid rubber and allowed to cure upside-down so that rubber does not drip along the length of the pin. This prevents thin spots from forming on the pin tips and later creating holes in the actuators. After the tip coatings are cured, the pins are dipped into liquid rubber or, in the case of larger assemblies, poured over with liquid rubber, taking care to obtain full coverage of the pin surfaces. Once fully coated, the pin assembly is left at room temperature to cure with the pins pointing upward. The purpose of curing at room temperature is to allow ample time for the rubber to flow to a steady state and minimize variations in rubber thickness. After curing, another layer of rubber can be added to increase the overall actuator thickness. The thickness of an individual layer is determined by the balance of gravity, surface tension, and viscosity of the rubber used. Thinners and thickeners may be mixed into the uncured silicone rubbers to adjust this but

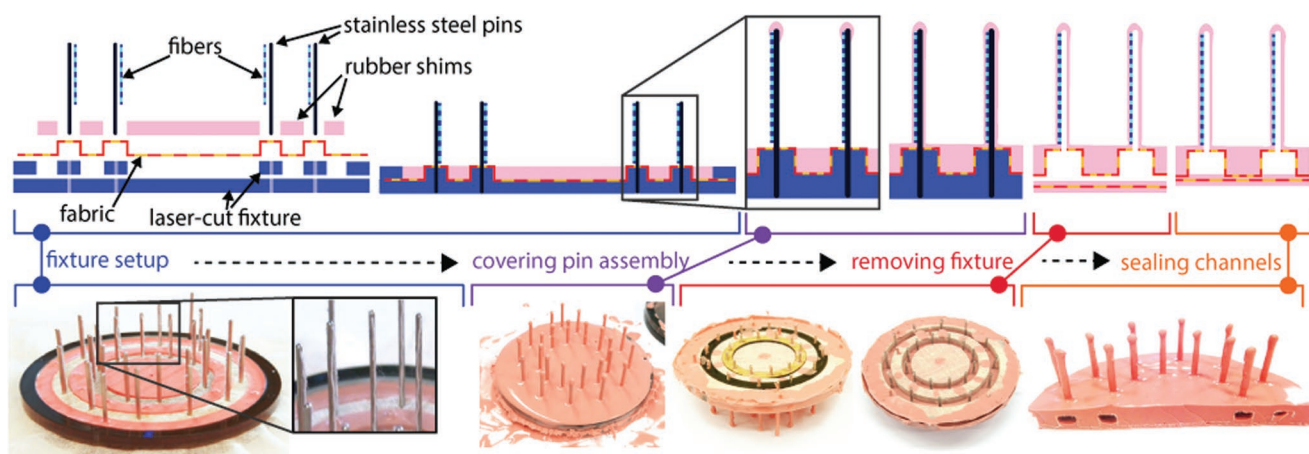


Figure 2. Overview of dip coating fabrication strategy including open face mold setup, dip coating results, mold removal, and sealing of pressure supply channels. Fibers are used for mechanical programming in this example and the resulting actuators bend toward the center of the assembly, in the direction of the fibers. The top row shows a schematic of the open faced mold assembly and dip coating with fiber inclusions, while the bottom row shows pictures of the dip coating process that correspond to the stages depicted in the schematics.

may also affect the stiffness and tear strength of the cured rubber. The pins can also be preheated or placed into an oven after dipping to speed up the curing time, thereby increasing viscosity soon after dipping, resulting in thicker layers. In order to limit the variables tested in this study, we chose to only vary the number of layers to control the outer diameter of the actuators.

Once the desired number of layers are added, the acrylic fixture and pins comprising the open face mold are removed and the resulting rubber structure can be sealed by pouring a thin sheet of liquid rubber over a piece of fabric and lightly pressing the open pressure supply channels into the liquid rubber. The fabric that was previously pinned between the rubber shims and base plate helps to mechanically anchor the previously cured rubber structure with the liquid rubber. Further detail of this process can be found in the Experimental Section and the Supporting Information.

While the dip coating and pour over techniques mentioned above are the fundamental methods used to create the arrays of soft structures presented in this work, a secondary component of the fabrication process is necessary in the creation of bending actuators to introduce an intentional structural bias that causes the soft structures to bend and curl when internally pressurized. This mechanical programming is accomplished with the use of fiber inclusions, gravity, surface tension, and electric fields to complement the forms created by the open face molds. A schematic of these modification methods is shown in **Figure 3** as well as cross-sections of soft actuators that were created with each method. A brief explanation of the four modification methods follows, and further details can be found in the Experimental Section and Supporting Information.

While exploring strategies for mechanically programming the soft actuators formed with open faced molds, modeling of similar soft actuators presented by Gorissen et al. provided a guide of advantageous design characteristics for the cross-sectional geometry. From their model, it is expected that bending actuators with larger internal diameters and high eccentricity will achieve the highest bending curvature for minimal stress in the material. The eccentricity is defined as the offset between the center point of internal void and the center of the external shape. This is, of course, inherently limited by the fact that the internal diameter and eccentricity of the structure should not create nonzero wall-thicknesses. Furthermore, wall thicknesses nearing zero pose higher fabrication challenges.^[31]

Gorissen et al. chose to constrain their analysis to actuators with a 1 mm outer diameter, while the variety of actuators in this work were constrained to a fixed inner diameter, as prescribed by the pins of the open faced molds. The guiding principle remains the same, though fabrication methods influenced which variables were constrained while exploring the design space. Further, while this model provides a valuable design guideline, the exploration in the work presented in this paper is predominantly focused on assessing manufacturing feasibility and the design space achieved by our new fabrication methods.

2.1. Actuation Direction Established via Strain-Limiting Fibers

Within an array of dip molded actuators, each individual actuator can be mechanically programmed to bend in an arbitrary direction with appropriately positioned strain limiting fibers in the fabrication process. An example array programmed with this method is shown in Figure 1A–D and an overview of the fabrication process, including the fiber incorporation, is shown in Figure 2. Encasing fibers into the side wall of the structures causes asymmetric stretching of the actuator when internally pressurized, thereby inducing a bending motion. A schematic of this mechanical programming method and a resulting cross-section can be seen in Figure 3A. This strategy is similar to larger scale soft actuators that use fiber reinforcements to program bending motions in pneumatic elastic actuators,^[20,32] as well as similarly scaled devices.^[17,33] To accomplish this, we lightly tack the fibers onto the open mold pins prior to inserting them into the mold form for dip coating. When the open face mold is dip coated or poured over, and the rubber cures on the pins, the fiber is mechanically incorporated into the side wall of the actuator, and releases from the pin when the mold assembly is removed. Due to surface tension, a side effect of the fiber on the side of the pin is that the wall thickness is greater on the fiber side of the actuator. This is visible in Figure 3A. The corners between the fiber and pin are also more likely to trap bubbles in the dip coating process and one such bubble is shown up close in Figure 3A. The greater thickness increases the stiffness of the actuator side wall, while bubbles reduce the stiffness, creating weak point if they are too large. These effects on stiffness, however, are second to the strain limiting effect of the fiber and we did not observe any failures from popping through bubbles trapped near the incorporated fibers.

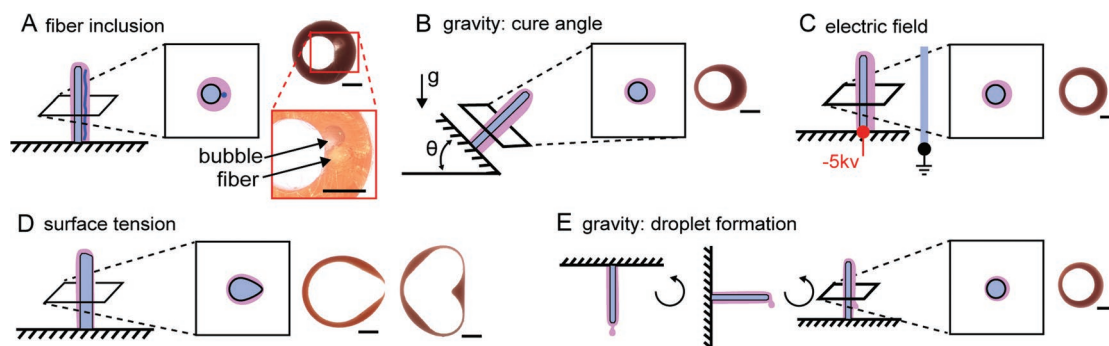


Figure 3. A–E) Schematics and cross-section examples of different methods of mechanical programming used with open face molds. The scale bars indicate 1 mm. The first cross-section shown in (D) is torn because the actuator ruptured in pressure testing prior to removing the cross section.

2.2. Unidirectional Actuation Established via Gravity

The use of gravity as a mechanical programming method is limited to unidirectional actuation, but it is also the least complex and least labor-intensive of the strategies presented in this work. As depicted in Figure 3B, the open face mold that has been dipped in liquid rubber is propped at an angle with respect to gravity during the curing process. As a result, more of the rubber drifts to the lower side of the pin, creating a thickness bias in the side wall of the actuator. When pressurized, the actuators will thus bend in the direction of the lower side because the thinner side wall inflates and stretches more than the thicker side. Given its simplicity, this method is convenient for constructing large arrays of actuators, such as the 256-part array shown in Figure 1E–H, as well as the construction of very high aspect ratio actuators like the one shown in Figure 4. In a prior demonstration of this mechanical programming strategy in the microtentacle created by Paek et al., the soft actuator was formed by curing rubber on a horizontal rod and later sealed after removal from the rod.^[21] In this work, curing angles ranging from 5° to 60° offset from vertical successfully produced bending actuators, though we focused on 30° to 60°. The open face mold creates a sealed actuator tip while also pneumatically coupling the actuators to the rest of the array.

An alternative strategy using gravity to create a structural bias in the open molding process, depicted in Figure 3E, uses droplets formed at the tips of an inverted open faced mold shortly after dip coating. The mold is then rotated 90° and the liquid silicone droplets shift to one side of the pin tips. The mold is then fully reverted such that the pins are pointing upward and the droplets then run down one side of the pins, leaving a thicker coating of rubber on one side.

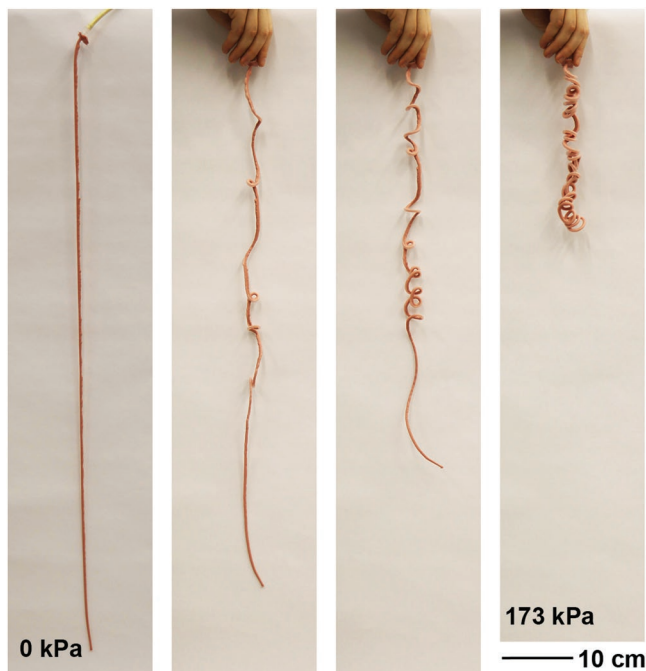


Figure 4. Inflation of an actuator that was formed on a 1.59 mm diameter, 1 m long pin.

2.3. Actuation Direction Established via Surface Tension

Similar to programming the bending motion of an actuator with fiber inclusions, the use of surface tension as a mechanical programming strategy allows for arbitrary arrangement of bending directions within an array of actuators. The bending motion is determined by biasing wall thickness through the use of pins with noncircular cross-sections. The cross-sectional profile of the pins is designed to leverage passive effects of surface tension on the liquid silicone to create thick and thin portions in the rubber coating. A schematic of this concept is shown in Figure 3D as well as images of cross-sections from two actuators. The interior profile of the actuator is defined by the pin shape while the exterior profile of the pin coating will tend toward a cross-section that minimizes the overall surface area, owing to surface tension acting on the liquid rubber. The pin geometry can thus be used to create thicker sections where rubber fills into concave pin surfaces, and thinner sections around features that protrude further and have tighter convex curvatures than neighboring features. We explored pin designs that focus on the creation of thick and thin features, and found that designs that leveraged convex protrusions to create thinner wall sections were more successful at achieving a bending motion through differential wall stiffness and greater curvature at lower actuation pressures. Additional pictures of pin designs and functional actuators can be found in the Supporting Information.

2.4. Actuation Direction Established via Electric Fields

The final method for mechanical programming makes use of static electricity to introduce a net charge into the liquid rubber-dipped pin. The pin is connected to a high voltage power supply and a nearby grounding electrode is used to attract the mass of the rubber off center with respect to the axis of the pin. This method does not allow for the creation of a fully arbitrary vector field of actuation, but does enable nonuniform actuation directions depending on the electrodes employed and electric field formed in the vicinity of the open faced molds. A schematic of this setup and a cross-section of a resulting actuator is shown in Figure 3C. In this work, demonstrations were limited to single pins and small arrays connected to a –5 kV potential, which are shown in the Supporting Information. Future work can be done to expand these into larger arrays, taking care to account for effects of multiple pins in the same electric field. To develop an understanding of the electric field acting on the rubber coating a single pin, a simulation of the electric field was made using an approximation of the pin as a point charge and the electrode as an infinite ground plane. Results from this simulation are shown in the Supporting Information.

2.5. Comparison of Mechanical Programming Strategies

The modification methods presented here have different advantages and disadvantages. The gravity method is the easiest to set up for large arrays in that any mold can be propped to a fixed angle while curing to accomplish the goal

of mechanical programming, but is limited in that all actuators will then bend equally in the same direction. Fibers allow for arbitrary direction selection but must be manually placed in the desired direction. This can be automated but is more time consuming when assembling by hand. Surface tension programming also allows for arbitrary direction arrangements and could provide variation in output curvature between different pins, as well as over the length of one pin, for a given input pressure by varying the pin shape. The surface tension strategy does, however, require custom pins, (though pins may be reused). The electric field programming can also support custom arrangements of actuation directions but this is limited by the complexity of electric field interactions as the number of charged pins increases.

Because the gravity and fiber programmed actuators achieved a higher burst pressure, tighter curvature, and higher engagement forces, we focused on these two methods for further exploration and characterization. The surface tension and electric field programmed actuators were not able to curl sufficiently to engage with some of the characterization tests described below but there is documentation of several functional examples in the Supporting Information. The surface tension method was limited to one or two dip coatings at the scale used for this exploratory work. The first and second coatings achieve the greatest differential in wall thickness and, as the pin geometry is covered by rubber, successive dip coatings add even layers and thus reduce the relative difference in wall thickness. Adjustments might be made to work around this and achieve a tighter curvature and higher engagement forces by exploring the use of different rubbers, alternative pin fabrication methods that would allow further geometry exploration that is not possible with the 3D printers used in this study, or multiple rubbers of varying stiffness to exaggerate the effect of the first layers while successive layers could just provide a soft skin to increase the overall thickness. Similarly, the electric field actuators were limited by a low differential in wall thickness, as is visible in Figure 3C. This differential could be enhanced with a stronger electric field by increasing the applied voltage, adjusting the electrode shape, moving the pins closer to the electrode, or doping the rubber with conductive materials to make it more responsive to the applied electric field.

2.6. Scale and Aspect Ratio Fabrication Limitations

To explore the size and aspect ratio limitations of this process, dip-coated actuators were made on pins ranging from 0.4 to 6.35 mm in diameter, and 6.35 mm in length, some of which can be seen in Figure 4 and Figure 5. Qualitatively, 0.4 mm was found to be challenging because the rubber starts to collect into droplets due to surface tension and these droplets significantly affect the function of the final actuator. The next size up, 1.59 mm, was found to reliably produce functioning actuators without the formation of droplets during the dipping and setup process. A small actuator diameter is appealing in the pursuit of high aspect ratios, lower bending moment, and higher packing density in arrays. Therefore, as the smallest reliable size, we used 1.59 mm pins to create actuators ranging

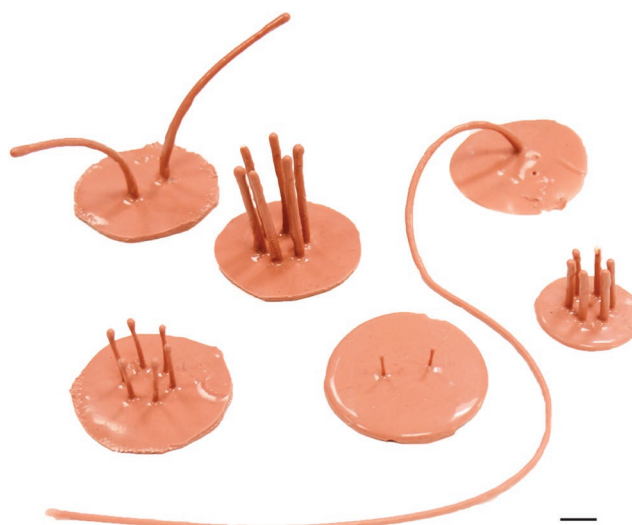


Figure 5. Demonstration of a range of aspect ratios achievable with variations on the dip coating fabrication method. The shortest actuator pictured is 6.35 mm long, and the longest is 30 cm. The scale bar in the image represents 1 cm.

from 6mm to 1m in length. Most of the process characterization was done with actuators formed on 38.1 mm long pins. These were chosen primarily by price point from the supplier and to have long enough actuators such they could bend completely back to themselves for characterizing bending radius versus operation pressure and to be able to curl fully around small objects.

The longest actuator fabricated for the purpose of this study was formed in three coatings on a 1 m long rod with a diameter of 1.59 mm, and cured at an angle of 45° to create a bias in the wall thickness. A picture of this actuator at several stages of inflation between 0 and 173 kPa is shown in Figure 4. After three coatings of rubber, the effective aspect ratio of the actuator was 200:1. The appropriate length and thus aspect ratio of a desired actuator will depend on the intended application. Actuators with embedded fibers were also fabricated up to 1 m in length, but the gravity programmed actuators were easier to demold and create a more consistent curling radius over the length of the actuator. Ultimately, the limiting parameters for the maximal aspect ratio are the curing time, viscosity, and surface tension of the rubber used.

3. Characterization of Actuator Performance

The characterization of the actuator arrays produced by the dip coating and programming strategies presented here was motivated by potential applications in manipulation of fluid flow and discrete objects, distributed grasping tasks, and locomotion. In the interest of these applications, the unconstrained curvature and holding force were measured for various fiber and gravity programmed dip coated actuators. The goal of these tests was to assess the sensitivity of actuator performance to fabrication parameters, including the number of dip coatings, the mechanical programming method, and variations within the programming method such as pin angle. In the case of pneumatic

actuators, one might want to tune a structure to bend a certain amount at a fixed pressure or tune a structure to have a specific threshold of engagement force. These tests are aimed to map a portion of the design space, as affected by fabrication variables, to allow intentional selection of the operating parameters.

Having a map of the operating pressures, resulting curvatures, and grasping forces is useful in selecting appropriate fabrication recipes to build actuators for an intended task. Another important consideration is matching to a suitable pneumatic power and control system that must be balanced with the operating parameters of the actuators. The internal pressures applied to each of the actuators was varied between the points when minimal pressure before deflection was observed up to failure by leaking or rupture. The results of these tests were used to inform fabrication parameters for the construction of the two arrays of actuators in Figure 1, as well as the high aspect ratio actuator in Figure 4. Following curvature and force characterization, a subset of the actuators were subjected to destructive testing. They were inflated to rupture to measure burst pressure and sliced to expose the cross-sectional distribution of thickness.

Smaller sample sets of operational pressure tests were also performed on actuators programmed with surface tension and electric fields but they were not subjected to grip force testing because they did not achieve a sufficiently tight curvature to hold on to the testing fixture. Further development of these mechanical programming strategies may enable greater curvature, otherwise they may only be used for applications that require less bending range, such as fluid flow manipulation. Actuation tests of the surface tension and electric field actuators are included in the Supporting Information.

3.1. Operational Pressure and Curvature Characterization

The unconstrained curvature was measured through a range of inflation pressures from the initial deformation up until the actuator curled onto itself. Tests were stopped when the actuator came in contact with its own base, or until the actuator leaked or burst before fully curling up. The curvature was measured with the help of a custom image processing script (Matlab, Mathworks) that tracked the edge of actuators in a series of pictures taken at various pressurization levels. Though the image tracking program was set up to find the inner and outer edge of the actuators, the outer edge was used for the curvature measurements below because it was more easily identified in the pictures by the tracking script due to the lighting in the pictures taken for this data set. **Figure 6** shows the curvature achieved at varying operating pressures for actuators mechanically programmed with fibers and gravity. The gravity-programmed samples represented in Figure 6 were cured at 30°, 45°, and 60° from level for the purpose of biasing the side wall thickness.

As may be expected, the most significant fabrication variable affecting the relationship between curvature and operating pressure is the number of dip coatings, and thus the overall thickness of an actuator. As shown in the plots in Figure 6, this manifests as discrete jumps between samples with different numbers of dip coatings, where the operational pressures shift higher with each coating. A notably higher operational pressure

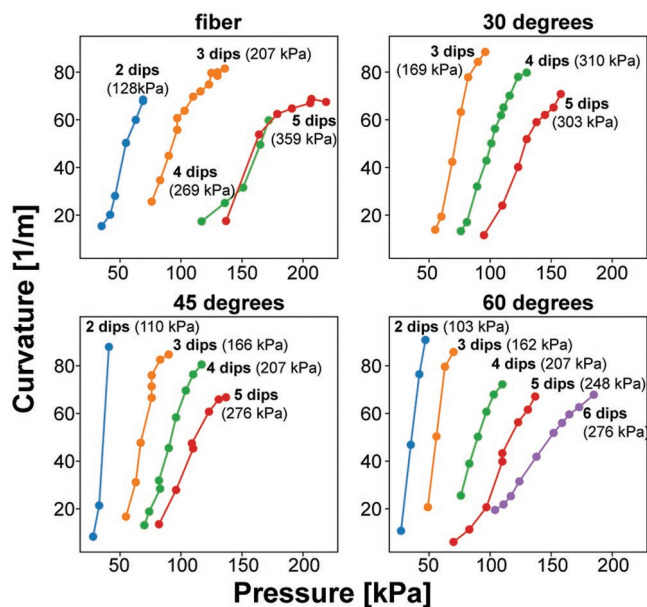


Figure 6. Plots of the curvature versus input pressure for actuators made with varying numbers of coatings and programmed with different gravity curing angles as well as fiber embedded actuators.

is also achieved through the incorporation of fibers into the dip coated structures versus the operating pressure of the gravity programmed structures. Among the gravity programmed actuators, their curing angle can be used to make finer adjustments to the operating pressures and the initial engagement pressure.

There is an unexpected overlap between two of the lines in Figure 6A. Using images taken during each of these pressure tests, we do not notice aberrant behavior of the actuators other than the fact that the five dip actuator begins to bend out of plane at higher pressures. Bending out of plane would register as an artificially higher curvature in the tracking script. Adjusting for this might move the five dip line downward but does not fully explain the fact that the two, three, and five dip actuators set a pattern that the four dip actuator does not closely follow. From this data and our experience in building these actuators, we draw the conclusion that there is some uncontrollable variance in the fiber programming method due to the hand-placement of the fibers. This may be improved with automation as well as the sourcing of straighter fibers. (The fibers used were unwound from cotton twine to achieve the desired diameter and thus have a residual helical shape that is difficult to straighten.) We do not expect the small variations to be problematic when averaged over large arrays, and the accuracy can be improved if necessary. Another option is to use the gravity programming approach for a higher degree of accuracy and consistency. This also influenced our decision to use the gravity programming method for the largest array and longest actuator prototypes, which benefit from a higher degree of consistency.

3.2. Holding Force Characterization

In the interest of gauging the potential for grasping, manipulation, and attachment with these fluidic bending actuators, their

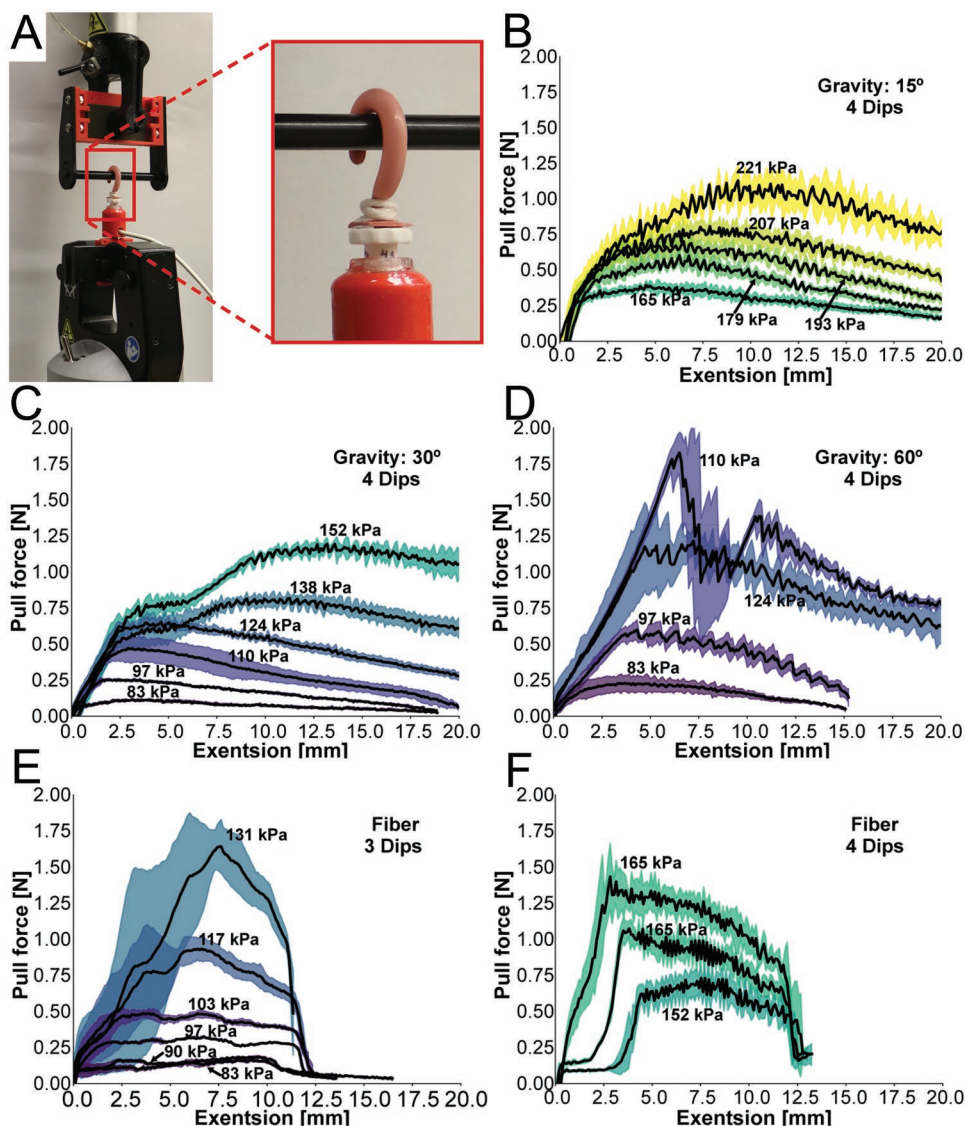


Figure 7. A) Picture of the fixture used in the Instron testing machine to perform holding force experiments. B–F) Example results from holding force tests. The center line represents the average value of five tests and the colored band is one standard deviation above and below average. The inflation pressure is labeled directly for each line and also corresponds to the color. The actuators represented include gravity programmed samples with four dip coatings and cured at a B) 15°, C) 30°, and D) 60° angle. Plots are also shown for fiber programmed actuators with E) three and F) four dip coatings. Additional data can be found in the Supporting Information and a plots of maximum holding forces values for actuators made with four dip coatings are summarized in Figure 8.

holding force was evaluated by measuring the force required to pull a 6.35 mm diameter rod out from an encircling actuator with varying internal pressurization values. These tests were performed on an Instron material testing machine with the setup shown in Figure 7A. Examples of holding force measurements for five individual actuators with different fabrication parameters are shown in Figure 7. The first three example actuators represented in the plots in Figure 7 were made with four dip coatings and mechanically programmed by curing at inclines of 15°, 30°, and 60°. The last two example actuators in Figure 7 were programmed with a fiber inclusion and made with three and four dip coatings. Each black line on the plots represents an average value of five trials and the shaded colored line represents one standard deviation above and below the

average value. The oscillations in the line are due to the stick slip interaction between the actuator and the rod as they slip past each other. A summary of the maximum average holding forces observed for actuators with four dip coatings and various mechanical programming parameters is shown in Figure 8. Similar individual actuator test results from additional actuators of varying dip coating layers and programming parameters can be found in the Supporting Information.

From the results shown in Figures 7 and 8, it can be seen that the force output is affected by the fabrication parameters, as well as the relationship between curvature and input pressure. In other words, a higher input pressure does not automatically translate to higher holding forces. The results in these figures show that increasing the pressure in a given actuator

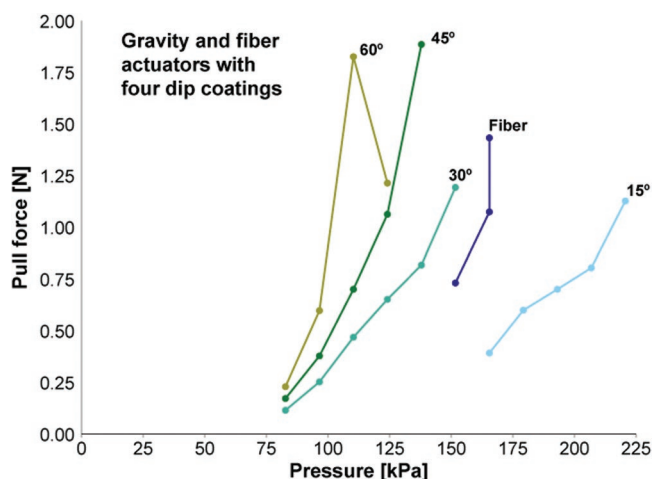


Figure 8. Overview of pull test data for actuators with four coatings. Each point represents the maximum average value of a set of five pull test trials, such as the ones shown in Figure 7.

will generally lead to an increased pull force, but a different actuator recipe may be able to achieve the same pull force with more or less internal pressure. Comparing this information to the curvature data shown in Figure 6 suggests that the relationship between operating pressure and curvature has an effect on the holding capacity of an actuator, likely related to the size of the object being grasped in relation to the enclosing geometry formed by the actuator.

The force applied to the rod as it is pulled away from the encircling actuator is largely dependent on the friction force between the actuator and the rod, which is affected by the actuator curl and the local contact shape. As would be expected, actuators that do not fully curl around the rod cannot apply an appreciable force in this test. As the rod is pulled out of the encircling actuator, the actuator is extended upward and uncurled, which results in a reduced holding force. When uncurled, a more distal portion of the actuator is in contact with the rod, creating a more compliant path between the rod and base of the actuator. As the actuator uncurls, there is also less engagement with the rod, resulting in lower friction between the two. The shape of the test curve is also affected by the initial curvature of the actuator, as determined by the inflation pressure and fabrication parameters. In cases like Figure 7F, the actuator is maximally curled around the rod at the start, whereas Figure 7B,C shows a trend that suggests that the actuator becomes better seated with a small amount of extension. We see that the holding force decreases as the actuator nears its fully uncurled extent in all of the plots in Figure 7. Artifacts on the inner surface, such as bumps from underlying fibers, as well as the tension in the actuator skin can also affect the measured grip force. When the actuator is fully curled but still compliant, the surface of the rubber conforms and sticks to the rod. By contrast, when an actuator is maximally pressurized, the surface conforms less to the rod and does not achieve that same adhesion. A fully pressurized actuator also provides greater resistance to uncurling and will sometimes instead twist sideways and slip off the side of the rod without fully uncurling. We believe these effects at higher pressures are connected to the downward trend seen

in the upper pressures in Figure 7D. A sequence of pictures of the extension process and additional holding force plots are included in the Supporting Information.

The holding forces achieved by the actuators built in these studies ranged from 0.25 to 2 N. While these are relatively small forces, one could increase the holding capacity of a system by employing similar actuators working in parallel. It may also be possible to increase engagement with longer actuators, like the one pictured in Figure 4, to achieve greater holding forces. By spreading holding contacts across an array of actuators, it may also be possible to minimize all contact forces while simultaneously increasing the overall holding capacity.

3.3. Burst Pressure

After operational pressure testing and holding force tests were performed, individual actuators were pressurized to the point of failure by bursting. In each case, the failure point was a rupture in the thinner side of the actuator wall, near the base. Intuitively, this was expected because the actuators are formed as a seamless body and the weakest point undergoing the most strain is the thinner side wall a couple millimeters above where the actuators is attached to a barb fitting. The rubber covering the base of the pin tends to be slightly thinner due to surface tension and gravity. A picture of this is shown in the Supporting Information. The cotton twine fixing the actuator to the barb covers this thin spot and also constrains extension of the rubber. This edge effect leads to a higher combination of axial and radial strain and thus creates the most probable failure point.

Burst pressure values for the actuators represented in Figure 6 are shown in parentheses, next to the line labels. A table of burst pressure values is also included in the Supporting Information. Burst pressure values ranged from 103 to 448 kPa for gravity and fiber programmed actuators with two to six dip coatings. As expected, burst pressures increased with the number of dip coatings. Within sets of actuators of the same number of dip coatings, gravity programmed actuators formed at low tilt angles and fiber programmed actuators had the highest burst pressure. Burst pressures decreased with increasing tilt angles, related to the fact that larger tilt angles lead to a greater difference between the wall thickness on either side of the pin and smaller wall thicknesses on the upper side of the dip coated pins overall.

In all fiber programmed and gravity programmed actuators at tilt angles of 30°, 45°, and 60°, the actuators were able to curl to their full extent, which was limited by the point at which the actuator tip made contact with the base of the actuator. Gravity programmed actuators fabricated at tilt angles of 15° and three, four, and five dip coatings were able to curl to their full extent, while those with two coatings only curled up to 180°. A six coat actuator at 15° was not tested.

4. Conclusion

This paper introduces a fabrication strategy for using open faced molds to create large arrays and high aspect ratio soft

actuators. It also describes four ways to modify those structures in the forming process in order to intentionally bias molding thicknesses or incorporate strain-limiting fibers. The thickness bias and fibers are then leveraged to mechanically program these soft structures to function as pneumatic bending actuators. Depending on the strategy chosen, actuators fabricated in integrated arrays may all bend in the same direction or can be prescribed an arbitrary vector field of bending directions. The achievement of long individual actuators as well as large integrated arrays of actuators is facilitated by the simplicity, low precision requirements, and low cost of the open face molding techniques that we present. We demonstrate a 1 m long actuator, as well as a 256-part array but believe that these processes could produce longer actuators and larger arrays, if desirable. The primary limitations on the length of actuators will be the available space and encumbrance of working with large rods making it difficult to maneuver, the sag in the rod when tilted over a longer distance creating a variation in the tilt angle, and the mix viscosity and cure time of the rubber limiting the ability of the rubber to flow and fine out to an even coating before the viscosity increases due to the onset of curing. The use of laser cut acrylic mold parts also allows for rapid generation and iteration of mold designs at low cost. The designs can also be created and edited as relatively simple, 2D designs in vector graphics software.

Future work with these fabrication methods could include exploring strategic actuation patterns or vector fields of bending motion direction mapped into large arrays of these actuators for the purpose of fluid manipulation, object manipulation, gentle grasping, and locomotion. A continuation of this work would also include the combination of multiple mechanical programming strategies in a single array or varying the parameters over the length of the pin to create purposeful variation in the bending profile. The programming methods utilizing surface tension and electric fields in particular may have a relatively low increase in manufacturing complexity to program variations in the bending profile over the height of the finished actuator. The pin cross section and proximity of electrodes could be varied along the length of the pin. Potential areas of exploration for the electric field strategy more specifically might also include placement of arrays of pins to intentionally affect the resulting electric field that biases the actuator thickness. The charging setup could also be modified to incorporate multiple charge states, such that the dipping mold could be segmented into different charge patterns that cycle at a frequency that allows two or more distinct electric fields to affect subsets of the forming actuators. More broadly, the open face molding strategies can also be further developed to incorporate these arrays onto nonflat architectures as well underlying functional structures that might allow for active morphology changes, such as an array of grasping cilia built onto a soft hand or tentacle designed to securely and gently pick up items.

5. Experimental Section

The actuators in this work were made from silicone rubber, Elastosil m4601 (Wacker Chemie) because of its high elongation to failure

(700%), high tearing force, and relatively low cost. The open faced dip coating molds were fabricated with laser-cut acrylic and stainless steel pins (McMaster-Carr PN90145A427). The fabrication process was also successfully reproduced with pins and molds made from varying plastics, including polyethylene, Teflon, and Delrin. The rubber does not stick to these materials and, once cured, they can be removed without the use of mold release. This is important to avoid mixing mold release into the liquid rubber, which would create a risk of thin spots and holes in the sidewalls of the actuators. While all of these materials successfully produced actuators, acrylic was used for mold structures because of its ease of laser-cutting and stainless steel pins were selected for their ability to rigidly hold their form, thus making it easier to assemble large, well-aligned arrays of pins that could be temporarily press-fit into a laser-cut acrylic fixture. For all variations of the fabrication process other than fabricating the actuators on the meter-long pins, the tips of the pins were dipped in rubber and allowed to cure before applying the first full coating. Without this step, the actuator tips would be too thin, resulting from gravity and surface tension affecting the rubber distribution.

Fiber Inclusion Preparation: To incorporate fibers into the actuator side walls, the fibers were lightly tacked onto the open mold pins prior to dip coating. A small amount of silicone glue (Silpoxy, Smooth-on) was used for the tacking because it can be incorporated into the final actuator structure. Cotton fibers were found preferable because they have a high surface area for better mechanical integration into the liquid rubber. For the demonstrations shown in this paper, a cotton twine (McMaster-Carr PN1929T12) was untwisted to isolate one of the plies. One of the plies was then cut to size, and tacked onto the pins.

Surface Tension Pins: The custom pins used for the surface tension experiments were printed on a Formlabs Form 2 printer in the clear resin (RS-F2-GPCL-04, Formlabs). This printer and plastic were chosen because it had sufficiently high print resolution and the printed pin could be pulled from the cured Elastosil M4601 rubber without the use of mold release. Furthermore, the printed parts did not inhibit the rubber from curing, as was the case with parts printed with Stratasys resins. Other silicone rubbers were tested with molds created with Formlabs resins, including Reynold's Dragon skin, smoothsil, and ecoflex series. The use of Elastosil M4601 was chosen for reasons mentioned above, but it also released from the Formlabs resin without mold release more easily than the other rubbers that were explored. The approximate pin diameters were increased from the 1.5 mm used in the other programming methods to 2–3 mm in order to achieve sufficient stiffness such that the pin could be printed with little to no support structure contacting, and thus marring, the molding surfaces. For larger production of custom pin forms, one could switch to injection molded or extruded plastic pins. This may also allow for smaller diameter pins than 3D-printing, if desirable.

Electric Field Setup: For the electric field setup, the same stainless steel pins mentioned above were press fit into a 3.18 mm thick acrylic disc with enough pin length protruding below the disc to be wrapped with a bit of bare copper wire and then pressed into a second acrylic disc. The purpose of the second disc was to ensure that the pin would be held up vertically. The copper wire was then connected to a power supply set to provide an electric potential of -5 kV. An aluminum plate, 0.2 cm thick, 3 cm cm tall, and 2 cm cm wide, was positioned 1.5 cm from the pin and connected to ground. This was successfully tested with the flat side of the plate most proximal to the pin as well as having the thin edge most proximal to the pin. The cross-sections and inflation tests shown are from the setup with the thin edge of the electrode positioned nearest to the pin in order to generate a stronger field concentration in the vicinity of the pin. A picture of the setup and pressurized actuators fabricated from this technique are included in the Supporting Information.

Process Modifications for Large Arrays and Long Actuators: To fabricate large arrays of actuators without requiring a large reservoir of rubber for dipping, rubber was poured over the top of the pins. Angling the mold for the purpose of using gravity to bias the wall thickness also allowed the rubber to be collected at the lower edge of the tilted mold and repoured. The formation of the longest actuators was still

accomplished via dipping but with a modified reservoir to reduce the amount of rubber wasted. A small cup with a hole in the bottom was raised to the top of the pin that was suspended from above, with the pin passing through the hole. The cup was filled with rubber while at the top of the pin and then pulled down the length of the pin. The direction of coating is important to ensure that the process is less sensitive to tolerance between the pin spacing and the vessel hole. For parallel fabrication of long actuators, a small laser-cut tray with multiple holes was used as a liquid rubber vessel. With this “infinite dipping vessel,” the limiting factors in the ultimate length that could be fabricated were rubber viscosity, surface tension, rubber curing time, and available space.

Mechanical Reinforcement and Layer Integration: Cotton cheese cloth (McMaster-Carr PN8808K11) was used to help mechanically anchor the layers of rubber forming the top and bottom of the pressure supply channels underneath the actuator array. The cheese cloth also limits the strain in the walls of the pressure supply channels. Cotton cloth was chosen to use as a means of mechanical anchoring in place of plasma bonding techniques to achieve higher strength with lower equipment requirements, and potentially less material and process sensitivity. The upper surfaces of the cheese cloth were incorporated into the first dip coated layer. As depicted in Figure 2, after the mold components were removed, the cheesecloth on the underside of the array was later used to mechanically bond the structure to a new layer of rubber that closed the bottom side of the pressure supply channels. The new layer was poured on a flat surface and the array was carefully pressed into the pool of liquid rubber and allowed to cure. A layer of cheesecloth was also incorporated into the bottom layer of the assembly to limit strain. Without this strain-limiting element, the support structure of the arrays may balloon in unwanted ways. In the array overview shown in Figure 2, the channels were then fully closed and a small hole was cut in order to insert an air supply. In some layouts, however, the channels were left open from the molding process and were sealed with silicone glue (Silpoxy). Another overview that includes this step as well as further information on fabrication methods can be found in the Supporting Information.

Supporting Information

Supporting Information is available from the Wiley Online Library or from the author.

Acknowledgements

This work was supported by the Office of Naval Research (Award #N00014-17-1-2063), the National Science Foundation Graduate Research Fellowship (under Grant #DGE1144152), and the Wyss Institute for Biologically Inspired Engineering. Any opinions, findings, conclusions, or recommendations expressed in this material are those of the authors and do not necessarily reflect those of the funding organizations.

Conflict of Interest

The authors declare no conflict of interest.

Keywords

arrays, dip molding, distributed contact, high aspect ratio, soft actuators

Received: October 28, 2019

Revised: December 13, 2019

Published online:

- [1] C. Y. Chen, L. Y. Cheng, C. C. Hsu, K. Mani, *Biomicrofluidics* **2015**, 9, 034105.
- [2] A. Keiřner, C. Brůcker, *Soft Matter* **2012**, 8, 5342.
- [3] B. Gorissen, M. de Volder, D. Reynaerts, *Lab Chip* **2015**, 15, 4348.
- [4] E. Milana, B. Gorissen, S. Peerlinck, M. De Volder, D. Reynaerts, *Adv. Funct. Mater.* **2019**, 29, 1900462.
- [5] F. Saito, K. Suzumori, in *2009 IEEE/RSJ Int. Conf. on Intelligent Robots and Systems (IROS 2009)*, IEEE, St. Louis, MO, USA **2009**, pp. 3025–3030.
- [6] A. R. Shields, B. L. Fiser, B. A. Evans, M. R. Falvo, S. Washburn, R. Superfine, *Proc. Natl. Acad. Sci. USA* **2010**, 107, 15670.
- [7] M. Vilfan, A. Potocnik, B. Kavcic, N. Osterman, I. Poberaj, A. Vilfan, D. Babic, *Proc. Natl. Acad. Sci. USA* **2009**, 107, 1844.
- [8] H. Lu, M. Zhang, Y. Yang, Q. Huang, T. Fukuda, Z. Wang, Y. Shen, *Nat. Commun.* **2018**, 9, 3944.
- [9] Y. Wang, J. Den Toonder, R. Cardinaels, P. Anderson, *Lab Chip* **2016**, 16, 2277.
- [10] K. Ogura, S. Wakimoto, K. Suzumori, Y. Nishioka, in *2008 IEEE Int. Conf. on Robotics and Biomimetics*, IEEE, Bangkok, Thailand **2009**, pp. 462–467.
- [11] S. Wakimoto, K. Ogura, K. Suzumori, Y. Nishioka, in *Proc. of IEEE Int. Conf. on Robotics and Automation*, IEEE, Kobe, Japan **2009**, pp. 556–561.
- [12] Y. Lu, C.-j. C. Y. Kim, in *12th Int. Conf. on Transducers, Solid-State Sensors, Actuators and Microsystems*, IEEE, Boston, MA, USA **2003**, pp. 276–279.
- [13] S. Konishi, F. Kawai, P. Cusin, *Sens. Actuators, A* **2001**, 89, 28.
- [14] O. C. Jeong, S. Konishi, *J. Microelectromech. Syst.* **2006**, 15, 896.
- [15] Y. Watanabe, M. Maeda, N. Yaji, R. Nakamura, H. Iseki, in *2007 IEEE 20th Int. Conf. on Micro Electro Mechanical Systems (MEMS)*, IEEE, Kobe, Japan **2007**, pp. 659–662.
- [16] S. Konishi, M. Nokata, O. C. Jeong, S. Kusuda, T. Sakakibara, M. Kuwayama, H. Tsutsumi, in *Proc. of IEEE Int. Conf. on Robotics and Automation*, Vol. 2006, IEEE, Orlando, Florida, USA **2006**, pp. 1036–1041.
- [17] N. R. Sinatra, T. Ranzani, J. J. Vlassak, K. K. Parker, R. J. Wood, *J. Micromech. Microeng.* **2018**, 28, aab373.
- [18] K. Suzumori, *Rob. Auton. Syst.* **1996**, 18, 135.
- [19] R. V. Martinez, C. R. Fish, X. Chen, G. M. Whitesides, *Adv. Funct. Mater.* **2012**, 22, 1376.
- [20] P. Polygerinos, Z. Wang, K. C. Galloway, R. J. Wood, C. J. Walsh, *Rob. Auton. Syst.* **2015**, 73, 135.
- [21] J. Paek, I. Cho, J. Kim, *Sci. Rep.* **2015**, 5, 10768.
- [22] D. Rus, M. T. Tolley, *Nature* **2015**, 521, 467.
- [23] B. T. Phillips, K. P. Becker, S. Kurumaya, K. C. Galloway, G. Whittredge, D. M. Vogt, C. B. Teeple, M. H. Rosen, V. A. Pieribone, D. F. Gruber, R. J. Wood, *Sci. Rep.* **2018**, 8, 14779.
- [24] R. V. Martinez, J. L. Branch, C. R. Fish, L. Jin, R. F. Shepherd, R. M. D. Nunes, Z. Suo, G. M. Whitesides, *Adv. Mater.* **2013**, 25, 205.
- [25] M. Cianchetti, M. Calisti, L. Margheri, M. Kuba, C. Laschi, *Bioinspir. Biomim.* **2015**, 10, 035003.
- [26] I. Must, E. Sinibaldi, B. Mazzolai, *Nat. Commun.* **2019**, 10, 344.
- [27] S. Kurumaya, H. Nabae, G. Endo, K. Suzumori, *Sens. Actuators, A* **2017**, 261, 66.
- [28] J. Zhou, S. Chen, Z. Wang, *IEEE Rob. Autom. Lett.* **2017**, 2, 2287.
- [29] K. C. Galloway, K. P. Becker, B. Phillips, J. Kirby, S. Licht, D. Tchernov, R. J. Wood, D. F. Gruber, *Soft Rob.* **2016**, 3, 23.
- [30] C. Lefteri, *Making It: Manufacturing Techniques for Product Design*, 2nd ed., Laurence King Publishing, London, UK **2012**.
- [31] B. Gorissen, W. Vincentie, F. Al-Bender, D. Reynaerts, M. De Volder, *J. Micromech. Microeng.* **2013**, 23, 045012.
- [32] K. C. Galloway, P. Polygerinos, C. J. Walsh, R. J. Wood, presented at *2013 16th Int. Conf. on Advanced Robotics (ICAR)*, IEEE, Montevideo, Uruguay, March **2013**.
- [33] A. Yamaguchi, K. Takemura, S. Yokota, K. Edamura, in *Proc. of IEEE Int. Conf. on Robotics and Automation*, IEEE, Shanghai, China **2011**, pp. 5923–5928.